On $Sr_{1-x}Na_xSiO_{3-0.5x}$ New Superior Fast Ion Conductors.

Ivana Radosavljevic Evans*, John S. O. Evans, Heather G. Davies, Abby R. Haworth and Matthew L. Tate

[1]Department of Chemistry, Durham University, Science Site, South Road, Durham, DH1 3LE, U.K.

Very high oxide ion conductivity in Na-doped $SrSiO_3$ materials $Sr_{1-x}Na_xSiO_{3-0.5x}$ ($0 < x \leq 0.45$) has recently been claimed, making these materials promising candidate electrolytes for intermediate temperature solid oxide fuel cells. We demonstrate, by a combination of laboratory powder X-ray diffraction (PXRD), powder neutron diffraction (PND), impedance measurements, SEM, ^{29}Si solid state NMR and quantification of amorphous content by Rietveld analysis, that the materials with these nominal compositions are two-phase mixtures containing one crystalline phase and a significant amorphous component. No significant Na doping into $SrSiO_3$ and hence no significant levels of oxide vacancies are found from Rietveld analysis of high-resolution neutron diffraction data. Conductivity of the samples increases systematically with increasing amorphous content, suggesting that the glassy phase is responsible for the conductivity observed rather than single-phase $Sr_{1-x}Na_xSiO_{3-0.5x}$ materials.

Recent report of very high oxide ion conductivity in K- and Na-doped $SrSiO_3$ by Singh and Goodenough has placed these materials at the forefront of the search for promising candidates for electrolytes in intermediate temperature solid oxide fuel cells (IT SOFCs).[1-5] The exceptional transport properties were correlated with neutron diffraction based conclusions that K and Na get stoichiometrically doped into $SrSiO_3$, creating large numbers of O^{2-} vacancies and giving rise to oxide ion conduction.[4] Most recently, excellent performance of the $Sr_{1-x}Na_xSiO_{3-0.5x}$ (x=0.45) composition in a fuel cell was reported.[6] However, a very recent publication on related K- and Ge-doped $SrSiO_3$ (which we became aware of during the final preparation of this manuscript), reported a direct investigation of oxide ion diffusivity of a nominal $Sr_{0.8}K_{0.2}Si_{0.5}Ge_{0.5}O_{2.9}$ composition by Isotope Exchange Depth Profiling (IEDP) and Time-of-Flight Secondary Ion Mass Spectrometry (ToF-SIMS), which found no evidence of O^{2-} diffusion. In addition, sub-micron elemental mapping revealed a chemical inhomogeneity of the sample.[7]

Our work has focussed on a systematic study of Na-doped $SrSiO_3$ materials (nominally $Sr_{1-x}Na_xSiO_{3-0.5x}$, x=0; 0.1; 0.2; 0.3; 0.4) by a combination of laboratory powder X-ray diffraction (PXRD), variable temperature powder neutron diffraction (PND), impedance measurements, SEM, ^{29}Si solid state NMR and the quantification of amorphous content by Rietveld analysis. We conclude that $x \leq 0.4$ samples contain significant amorphous material and far lower Na content than believed to-date.

Laboratory PXRD and impedance measurements were used initially to confirm that the our Na-doped materials were similar to those reported previously.[2] Bragg peaks in PXRD patterns suggest all samples are single phase materials, and could be fitted using the $SrSiO_3$ structural model.[8] Fig. 1 shows the conductivity *vs.* reciprocal temperature Arrhenius plot for $Sr_{1-x}Na_xSiO_{3-0.5x}$, $0 \leq x \leq 0.4$, samples, as well as the values reported for the nominal x=0.4 composition by Singh and Goodenough.[2] We note that the latter are about one order of magnitude higher; the same potential inconsistency was observed by Bayliss *et al*. for the K/Ge-system. [7]

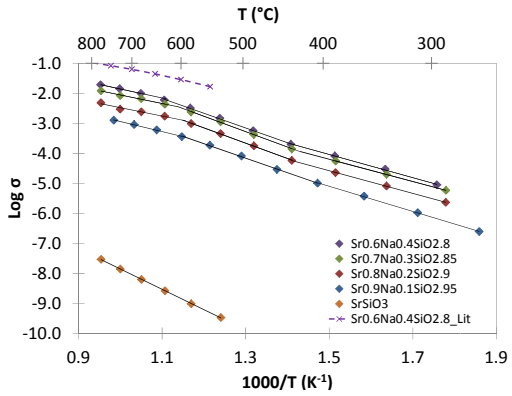

Figure 1. Conductivity *vs*. reciprocal temperature plot for the nominal $Sr_{1-x}Na_xSiO_{3-0.5x}$ ($0 \leq x \leq 0.4$) samples.

Neutron diffraction data collected at HRPD at the ISIS facility on samples with x=0.2, 0.3 and 0.4 were analysed by Rietveld refinement.[9, 10] Experimental details are given as Supplementary Information; the quality of the refinements is illustrated in Fig. 2 (full size in Fig. S3).

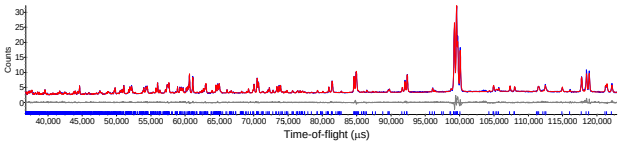

Figure 2. Rietveld fit obtained for the nominal $Sr_{0.6}Na_{0.4}SiO_{2.8}$ composition using high resolution ND data; R_{wp}=2.299%.

The starting model used was the monoclinic $SrSiO_3$ structure reported by Nishi.[8] Refinement of Na occupancies on the two Sr sites (with the total site occupancy constrained to 1, but without any restraints on the amounts of Sr and Na) and free refinement of the fractional occupancies of five O sites gave compositions $Sr_{1.01(2)}Na_{-0.01(2)}SiO_{3.00(2)}$ and $Sr_{1.02(2)}Na_{-0.02(2)}SiO_{3.02(2)}$ for the x=0.2 and 0.3 samples, respectively; for the x=0.4 sample, the content refined to $Sr_{0.94(2)}Na_{0.06(2)}SiO_{2.98(2)}$. We therefore conclude that the amount of Na doped into $SrSiO_3$, if any, is significantly below the nominal composition. Consequently, the level of O^{2-} vacancies created is far below that believed to-date, suggesting that O^{2-} ion conduction *via* vacancy-hopping mechanism is unlikely in these materials. Furthermore, these refinements indicate that the bulk of Na must be present in a second, amorphous, phase.

SEM images of Na-doped samples support the presence of two phases; Fig. S2 shows the nominal $Sr_{0.6}Na_{0.4}SiO_{2.8}$ composition. EDX data showed very low Na content in the Sr-containing phase, and high Na content in the second phase. Fig. 3 shows the ^{29}Si solid state NMR spectra for samples with increasing Na content. The spectrum of $SrSiO_3$ (shown in Fig. S4) contains a single resonance with a chemical shift of -84.9 ppm, the signature of the Si_3O_9 rings present. For $x > 0$, a second broad resonance appears and increases in intensity with x.

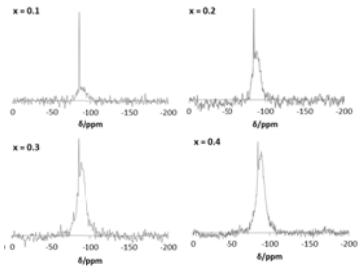

Figure 3. ^{29}Si solid state NMR spectra of $Sr_{1-x}Na_xSiO_{3-0.5x}$, 0.1; 0.2; 0.3; 0.4.

The broad feature represents Si in a range of environments typical of amorphous phases. Relaxation measurements strongly suggest that the sharp and the broad resonance originate from two different phases. The broad feature which relaxes very quickly (T_1 < 1s) is consistent with a glass, while the sharp line with a much longer T_1 (~ 90 minutes) is consistent with a crystalline phase.

The observations from Rietveld refinements of our apparently single phase samples containing little Na, coupled with solid state NMR and SEM data, suggest that significant quantities of amorphous material must be present. For zero Na doping into $SrSiO_3$, the formal reaction

$Sr_{1-x}Na_xSiO_{3-0.5x} \rightarrow (1-x)\ SrSiO_3 + x/2\ Na_2Si_2O_5$

implies 27 wt% of amorphous material for x=0.4. We have used quantitative Rietveld analysis to determine the amorphous content of our samples by mixing with a known mass of a crystalline phase. To minimise effects of micro-absorption and other systematic errors we chose Si as an internal standard and samples were micronised before measurement. Measurements performed on the x=0.4 sample with 5 different concentrations of Si gave an amorphous content of 33(4) wt%. Measurements were also performed on a series of samples deliberately diluted with additional quantities of amorphous SiO_2 in addition to a 20% Si spike phase. Extrapolation back to zero additional components gave an amorphous content of 26(2) wt%. Both methods give amorphous content consistent with no significant Na doping. Fig. 4 shows amorphous content determined using a 20 wt% Si spike for samples with x=0.1 to x=0.4. Extrapolation to x=0 shows low 5(2) wt% content for hypothetical x=0 material with the monoclinic structure. The dashed line gives the amorphous weight percent expected if all the Na were present in the amorphous phase. The similarity in slope of the experimental and predicted lines gives strong support to the hypothesis that the bulk of the Na is present in an amorphous material for all samples.

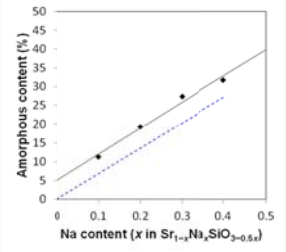

Figure 4. Amorphous content in $Sr_{1-x}Na_xSiO_{3-0.5x}$, x=0.1; 0.2; 0.3; 0.4. The dashed line gives the wt% expected if all the Na were present in an amorphous phase.

For x=0, our powder diffraction data revealed some discrepancies between the observed pattern and that calculated from the existing structural model. Non-zero intensities are predicted by the monoclinic $SrSiO_3$ model at positions where no peaks were observed in the PXRD and ND patterns (though weak broad features were observed at similar 2Θ) (Figs. S1 and S5). Indexing of the PXRD pattern showed that all peaks could be accounted for by a trigonal unit cell with cell parameters a=4.12 Å c=10.12 Å and V=148.88 Å^3, while systematic absences suggested possible space groups P31c and P-31c. The trigonal and the monoclinic cells are related: a_t=1/3 a_m, b_t=√3/3 b_m, c_t=c_m and V_t=1/6 V_m. Based on this relationship, the $SrSiO_3$ structure was solved by inspection in space group P-31c and refined against XRD and high-resolution ND data. The final Rietveld plots (Figs. 5 and S6) show excellent agreement for all but two weak peaks in the neutron data (~ 1.23 and 1.02 Å); these may arise from a small percentage of a Si-rich phase needed for compositional balance. Rietveld fitting of ND data for the x=0.1 sample gave a ~50:50 mix of the trigonal and monoclinic forms.

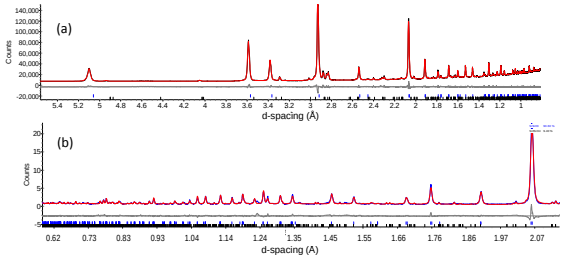

Figure 5. Rietveld fits obtained for trigonal $SrSiO_3$; overall R_{wp}=4.912%. (a) PXRD (R_{wp}=2.243%); (a) ND (R_{wp}=8.515%).

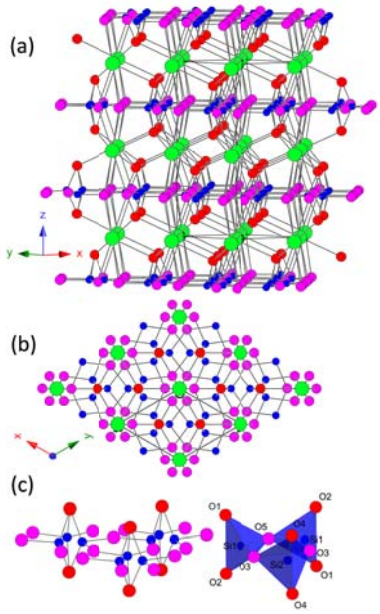

Figure 6. Trigonal structure of $SrSiO_3$. Green spheres are Sr, blue spheres Si, red spheres terminal O atoms and pink spheres bridging O atoms in Si_3O_9 groups. (a) Layers stacked along the c-axis. (b) View down the c-axis. (c) Ordered Si_3O_9 groups in the monoclinic structure (right) and disorder of Si and the bridging O atoms in the trigonal structure (left).

The $SrSiO_3$ structure in space group P-31c is closely related to the monoclinic structure. Both contain layers of edge-sharing SrO_8 groups which stack along the *c*-axis (Fig. 6a), alternating with layers of Si_3O_9 groups made up of corner-sharing SiO_4 tetrahedra. In the monoclinic structure, the silicate groups are ordered, whereas in the trigonal structure they are statistically disordered over three equivalent positions, Figs. 6b and 6c. There is presumably local ordering of these groups within the structure, but no long range order leading to monoclinic symmetry. We presume that formation of the trigonal form is a kinetic effect as it occurs for syntheses in the absence of Na where formation of $SrSiO_3$ is faster.

In conclusion, our materials with nominal compositions $Sr_{1-x}Na_xSiO_{3-0.5x}$, x=0.1; 0.2; 0.3; 0.4 have similar properties to those reported before but are mixtures containing a crystalline phase and a significant amorphous component. The amount of Na doped into $SrSiO_3$ is below the reliable detection limit of our high quality powder neutron diffraction. Quantification of amorphous content suggests that the bulk of the Na is present in the amorphous component. Conductivity of the samples increases systematically with increasing amorphous content, suggesting that a glassy phase is responsible for the conductivity observed, rather than single-phase $Sr_{1-x}Na_xSiO_{3-0.5x}$ materials.

ASSOCIATED CONTENT

Additional experimental and data analysis details are available as Supporting Information.

AUTHOR INFORMATION

Corresponding Author

ivana.radosavljevic@durham.ac.uk

ACKNOWLEDGMENT

The solid-state NMR spectra were obtained at the EPSRC UK National Solid-state NMR Service at Durham University. Dr. David Apperley is acknowledged for the data collection and assistance with interpretation of the NMR spectra. Dr. Leon Bowen is acknowledged for SEM. We thank Professor Arthur Sleight (Oregon State University) for useful discussions.

REFERENCES

1. Singh, P.; Goodenough, J. B., *Energy & Environmental Science* **2012,** 5, (11), 9626-9631.
2. Singh, P.; Goodenough, J. B., *Journal of the American Chemical Society* **2013,** 135, (27), 10149-10154.
3. Goodenough, J. B.; Singh, P. US 2014/0080019, 2014.
4. Martinez-Coronado, R.; Singh, P.; Alonso-Alonso, J.; Goodenough, J. B., *Journal of Materials Chemistry A* **2014,** 2, (12), 4355-4360.
5. Xu, J.; Wang, X.; Fu, H.; Brown, C. M.; Jing, X.; Liao, F.; Lu, F.; Li, X.; Kuang, X.; Wu, M., *Inorganic Chemistry* **2014,** 53, (13), 6962-8.
6. Wei, T.; Singh, P.; Gong, Y.; Goodenough, J. B.; Huang, Y.; Huang, K., *Energy & Environmental Science* **2014,** 7, (5), 1680-1684.
7. Bayliss, R. D.; Cook, S. N.; Fearn, S.; Kilner, J. A.; Greaves, C.; Skinner, S. J., *Energy & Environmental Science* **2014**.
8. Nishi, F., *Acta Crystallographica Section C-Crystal Structure Communications* **1997,** 53, 534-536.
9. Coelho, A. A.; Evans, J. S. O.; Evans, I. R.; Kern, A.; Parsons, S., *Powder Diffraction* **2011,** 26, (4), S22.
10. Rietveld, H. M., *Journal of Applied Crystallography* **1969,** 2, 65.